Cell, Vol. 109, 307–320, May 3, 2002, Copyright ©2002 by Cell Press

Coordinated Transcription of Key Pathways in the Mouse by the Circadian Clock

Satchidananda Panda,[1,4,7] Marina P. Antoch,[2,7,8] Brooke H. Miller,[2] Andrew I. Su,[1,3] Andrew B. Schook,[2] Marty Straume,[5] Peter G. Schultz,[1,3] Steve A. Kay,[1,4] Joseph S. Takahashi,[2] and John B. Hogenesch[1,6]

[1]The Genomics Institute of the Novartis Research Foundation
San Diego, California 92121
[2]Howard Hughes Medical Institute
Department of Neurobiology and Physiology
Northwestern University
Evanston, Illinois 60208
[3]Department of Chemistry
[4]Department of Cell Biology
The Scripps Research Institute
La Jolla, California 92037
[5]Department of Statistics
University of Virginia
Charlottesville, Virginia 22904

Summary

In mammals, circadian control of physiology and behavior is driven by a master pacemaker located in the suprachiasmatic nuclei (SCN) of the hypothalamus. We have used gene expression profiling to identify cycling transcripts in the SCN and in the liver. Our analysis revealed ~650 cycling transcripts and showed that the majority of these were specific to either the SCN or the liver. Genetic and genomic analysis suggests that a relatively small number of output genes are directly regulated by core oscillator components. Major processes regulated by the SCN and liver were found to be under circadian regulation. Importantly, rate-limiting steps in these various pathways were key sites of circadian control, highlighting the fundamental role that circadian clocks play in cellular and organismal physiology.

Introduction

Circadian rhythms are near-24-hour rhythms of biological processes that persist in the absence of environmental cues such as light and temperature. Such rhythms have been described in organisms ranging from photosynthetic prokaryotes to higher eukaryotes and reflect the existence of an underlying intrinsic circadian oscillator or biological clock (Harmer et al., 2001; Young and Kay, 2001). This circadian oscillator may impart an advantage to the organism by temporally orchestrating physiological and behavioral processes to better adapt to the predictable daily changes in the environment. For example, in cyanobacteria and *Arabidopsis*, the circadian oscillator directs transcription of the photosynthetic machinery to the daylight hours, thereby ensuring efficient assimilation of light energy. In mammals, circadian consolidation of locomotor activity to time of food availability and predator avoidance functions to improve survival.

The molecular mechanism of the circadian oscillator as a transcriptional-translational feedback loop has been unraveled by genetic analysis in *Drosophila* and mammals (King and Takahashi, 2000; Young and Kay, 2001). Two transcriptional activators, CLOCK and MOP3/BMAL1, regulate gene expression by interacting with enhancer elements termed E boxes. Target genes of these activators include several repressor proteins, including PER1, PER2, PER3, CRY1, and CRY2, which function to inhibit the CLOCK/MOP3 complex, thereby generating a circadian oscillation in their own transcription. Although the core molecular pacemaker is defined, the molecular outputs that ultimately regulate circadian control of cellular physiology, organ function, and systems-level behavior are poorly understood. Specifically, the link between circadian transcriptional output and physiology under circadian control has been lacking. Researchers have recently used high-density oligonucleotide arrays to discover transcripts with circadian expression patterns in young *Arabidopsis* seedlings, *Drosophila* heads, and rodents (Claridge-Chang et al., 2001; Grundschober et al., 2001; Harmer et al., 2000; Kita et al., 2002; McDonald and Rosbash, 2001). Such analysis in plants has identified hundreds of circadian-regulated genes, several transcription factors that control cycling transcription, and one *cis*-acting promoter element mediating cycling gene expression. Similar studies in *Drosophila* have identified a fewer number of cycling transcripts, perhaps reflecting the heterogeneity in fly heads that included a few lateral neurons, the relatively larger compound eyes, and a significant amount of fat bodies. Finally, temporal gene expression profiling of rat fibroblasts using high density arrays (HDA) (Grundschober et al., 2001), the kidney and liver using cDNA arrays representing a limited subset of rat ESTs (Kita et al., 2002), and differential display of mouse liver transcripts (Kornmann et al., 2001) have identified some novel circadian output genes.

In order to dissect how the master oscillator resident in the SCN functions to coordinate behavioral and physiological rhythms throughout the whole organism, we have used high-density oligonucleotide arrays to examine the expression of more than 7000 known genes and 3000 expressed sequence tags (ESTs) over two circadian days in the SCN and liver. Analysis of temporal patterns of expression revealed nearly 650 circadianly regulated transcripts, most of which cycle in either SCN or liver but not both. Included in this data set are many transcripts previously identified as circadianly regulated, thus validating our approach, along with many more genes and ESTs previously unknown to be regulated by the circadian oscillator. Analysis of expression patterns of these genes revealed transcriptional networks and targets that underlie temporal regulation of major functions of the SCN and liver. The observation

[6]Correspondence: hogenesch@gnf.org
[7]The first two authors contributed equally to this work.
[8]Present address: Department of Cancer Biology, Lerner Research Institute, The Cleveland Clinic Foundation, Cleveland, Ohio 44195.

that rate-limiting steps in several pathways are selectively regulated in the clock demonstrates that the circadian clock has evolved efficient mechanisms for its complex regulation of physiology. A comparison of these results with those recently published in fly revealed that the circadian regulation of several pathways and physiologies are conserved over 600 million years of evolution. Finally, we have constructed a publicly accessible database (http://expression.gnf.org/circadian) that users can query for circadianly regulated genes in the SCN or liver, or for the temporal expression patterns of their genes of interest.

Results and Discussion

We entrained C57BL/6J mice to a 12-hour light, 12-hour dark cycle (LD12:12) under constant temperature for two weeks, and then we transferred the mice to constant darkness. Starting at 30 hr after lights off, which corresponds to circadian time 18 (CT18), tissue samples were collected from ten mice every 4 hr for two complete circadian cycles. This strategy excluded light-regulated genes that are not under endogenous circadian control, while the second circadian cycle ensures a repeating pattern of 24 hr and serves as a replicate of the first day. For each time point, biotinylated cRNAs were prepared from pooled mRNA and hybridized to duplicate sets of high-density microarrays (HDAs) (Affymetrix, Palo Alto, CA) to minimize experimental error. Expression values for each gene were interrogated for circadian variation using a cosine wave-fitting algorithm, COSOPT, which is a modified version of a previously described algorithm CORCOS (Harmer et al., 2000). For each probe set (transcript), COSOPT performed an arithmetic linear-regression detrend of the original time series. In a two-stage analysis, the detrended data set was tested for fitness to cosine test waves with average periodicity of 24 hr (see Experimental Procedures). First, the data set was tested for fitness to several cosine test waves, and then the significance of fit (if any) was empirically tested. This process results in a multiple measures corrected β (MMC-β) value denoting the goodness of fit of the time course to a circadian pattern of expression (period and phase) that is independent of the amplitude of rhythmicity and is weighted for experimental error at each time point. This strategy precludes user bias for amplitude, accounts for hybridization variability, and accommodates a slight variability in period length. Transcripts whose traces fit a cosine wave with a period of between 20 and 28 hr with MMC-β value of $<$0.1 were considered circadianly regulated. This cutoff value was chosen based on two observations. First, comparison of MMC-β values for genes previously identified as circadianly regulated indicate that a cutoff value of 0.1 successfully identifies $\sim$75% of cycling genes (see Supplemental Table S4 and Supplemental Figure S1 at http://www.cell.com/cgi/content/full/109/3/307/DC1). To calculate the false positive rate, 1000 simulations were performed considering duplicate Gaussian random time series that simulated data collections from 0 to 48 hr at 4 hr sampling interval. Under these conditions, the false positive rate was below 1%. Taking into account the rising false positive rate as MMC-β values increase, we chose an MMC-β value of 0.1 to balance the false positive and false negative rates of COSOPT. Several genes previously identified as circadianly expressed, including *Cry1*, *Per2*, *Mop3*, *Ccr4* (nocturnin), *Cyp7a1*, *Alas1*, *Pacap*, and *Gad1* (glutamic acid decarboxylase 1), were scored circadian in the appropriate phase and tissue(s) in our data set, thus validating our strategy. Temporal expression patterns of many genes assayed either by in situ hybridization or real-time PCR further validated this approach. Some previously known circadian-regulated genes, including *Per1*, were apparently cycling but had a higher MMC-β (0.18 for *Per1* in the SCN), usually because the signal to noise for that probe set was low. Therefore, it must be noted that some genes that lie outside this conservative MMC-β cut-off value may be scored circadian by independent methods. For example, in situ hybridization has confirmed cycling of *Kcnma1* (MMC-β = 0.21) in the SCN (discussed below).

For this reason, we have presented our data in a publicly accessible database with active links to other public sources of gene annotation. The circadian database (http://expression.gnf.org/circadian) can be searched in a text-based query for temporal expression patterns of a given gene in the SCN or in liver or, alternatively, to find genes that meet a given MMC-β cut-off value. The output of the search is a graphical representation of the hybridization data along with an associated MMC-β value and gene annotation.

Circadian Gene Expression Is Tissue Specific

The availability of a comprehensive temporal gene expression data set from two different tissues offered an opportunity for a systematic analysis of circadian transcriptional outputs of the clock. We determined that about 650 genes were under circadian control in the SCN and liver (Figures 1A–1C; see Supplemental Tables S1 and S2 at http://www.cell.com/cgi/content/full/109/3/307/DC1.) The peak expression of these genes was distributed throughout the circadian cycle (Figures 1A and 1B), with CT10 (ten hours after subjective dawn) and CT22 having the most circadianly regulated transcripts in the SCN—roughly anticipating dusk and dawn (Figure 1C). In liver, the largest clusters of circadianly regulated transcripts occurred at CT14 and CT06 (Figure 1C), likely indicating the distinct temporal organization of the physiologies mediated by the liver.

Comparison of the overlap between cycling genes in the SCN and liver revealed only 28 genes in common (Figure 1D; see Supplemental Table S3 at http://www.cell.com/cgi/content/full/109/3/307/DC1). These genes included the oscillator component *Per2* as well as several genes whose transcripts were previously unknown to cycle. Transcripts that cycle in all tissues may represent basic circadian outputs of cellular physiology or components of the circadian oscillator itself such as *Per2*. As previously noted, most transcripts, including *Per2* and Rev-erb β, are delayed by 4 to 8 hr in peak expression in liver with respect to the SCN (Figures 1E–1G; Zylka et al., 1998). However, several were coordinately regulated to the same phase in both tissues, including tubulin β 5 (*Tubb5*), and a transforming growth factor β 1-induced transcript (*Tgfb1i4*). To further investigate the overlap in cycling genes between the SCN

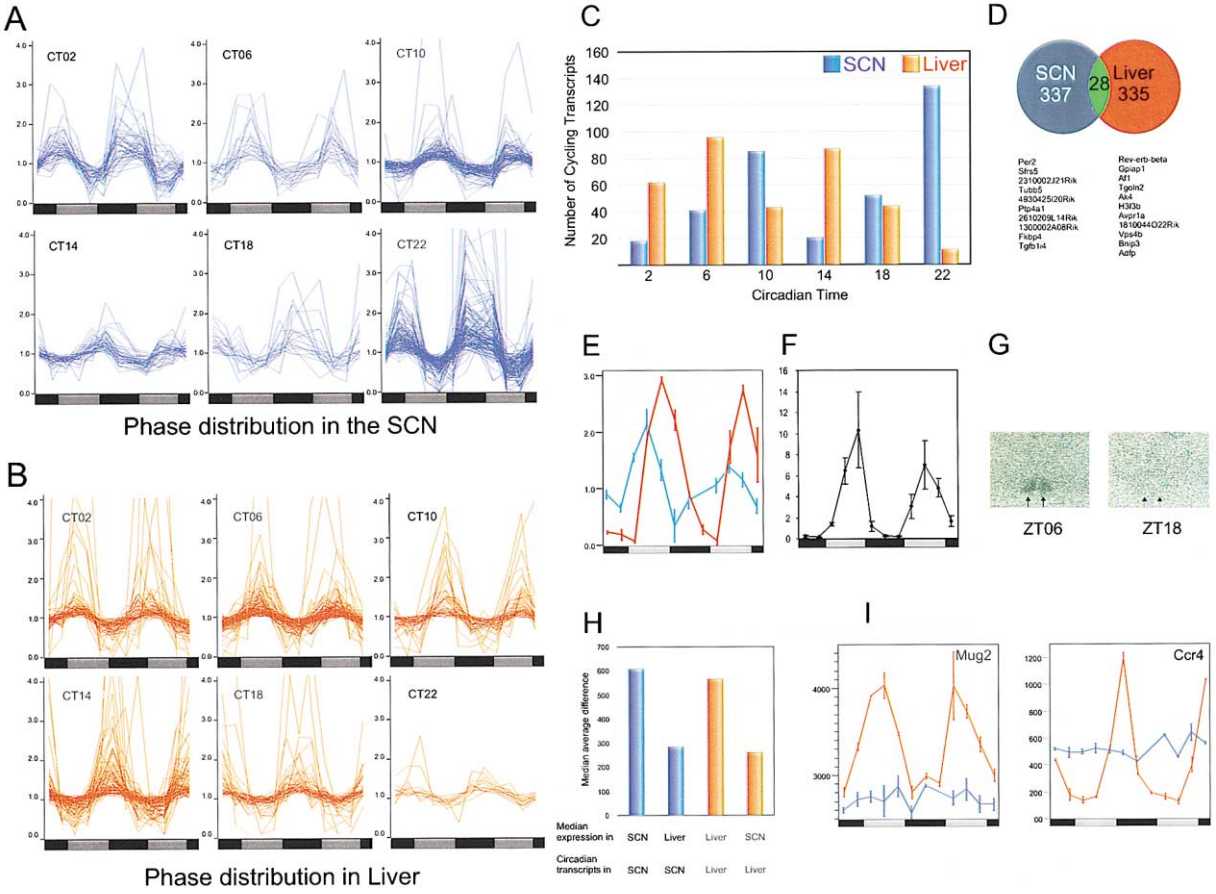

Figure 1. Circadianly Regulated Genes in the SCN and Liver

We determined 337 SCN and 335 liver transcripts to be circadianly regulated by COSOPT, and they were binned into six circadian phases, 2, 6, 10, 14, 18, and 22, by cluster analysis. Data traces of different phase clusters (A) in the SCN and (B) in liver. Expression patterns for these transcripts were visualized using Genespring (Silicon Genetics, Redwood City, CA). Data were normalized such that the median signal strength for each gene over all time points was 1. The average signal strength at each time point was then displayed as a ratio relative to the median signal strength of that gene. Values in the *x* axis represent hours after the first subjective dawn.

(C) Distribution of cycling transcripts in the SCN (blue bars) and liver (red bars) by circadian phase clusters.

(D) Cycling transcripts are tissue specific. Transcripts indicated as cycling (MMC-$\beta < 0.1$) were compared between SCN (blue) and liver (red) with transcripts cycling in both tissues indicated by the intersection (green) and listed below.

(E) Cycling of *Rev-erb*-β (U09504) in SCN (blue) and liver (red) was confirmed by (F) real-time PCR assays of liver samples and (G) SCN in situ hybridization (arrows point to the SCN). Mean $\pm$ SEM are shown in (E) and (F).

(H) Median expression levels of SCN circadian transcripts in the SCN and liver (in blue), and liver circadian transcripts in liver and in the SCN (red). A description of the distribution of median expression levels of these genes in the two tissue types and some examples are represented in Supplemental Figures S2 and S3 at http://www.cell.com/cgi/content/full/109/3/307/DC1.

(I) The expression patterns for *Mug2* (left) and for *Ccr4* (right) are shown with SCN expression indicated in blue and liver expression indicated in red. Mean average difference values $\pm$ SEM at each time point are shown.

and liver, we determined the median level of expression for cycling genes derived from either tissue in both tissues. This analysis revealed that in general cycling genes from one tissue have lower expression levels in the other (Figure 1H). In addition, a significant number of cycling genes in the liver or SCN are not expressed at detectable levels in the alternate tissue (Supplemental Figure S2). An example is murinoglobulin 2 (*Mug2*), whose expression is tightly restricted (and circadianly regulated) to the liver (Figure 1I; Lorent et al., 1994). Several other examples of the multiple tissue expression profiles of these genes (Su et al., 2002), along with their circadian expression profiles in the SCN or liver, are presented in Supplemental Figures S3A–S3J, which can also be accessed at http://expression.gnf.org. Other genes, such as carbon catabolite repression 4 homolog, *Ccr4*, are expressed at approximately the same levels in both SCN and liver, yet only cycle in the liver (Figure 1I). The previously described circadian expression pattern of *Ccr4* in several other peripheral tissues such as kidney, heart, spleen, and retina, but not in the SCN, highlights the tissue-specific component to circadian transcriptional rhythmicity in higher animals (Wang et al., 2001).

Such tissue-specific circadian regulation of transcription is a distinct feature of the circadian clock in higher organisms. In primitive unicellular organisms, the circadian oscillator directs transcription of a significantly

large portion of the genome in similar phase from cell to cell (Liu et al., 1995). In multicellular organisms, however, the clock may direct transcription of a small subset of genes in different organs relevant to the distinct function of that organ. A master oscillator resident in the SCN orchestrates circadian regulation in different organs to produce systems-level circadian changes in behavior and physiology to adapt to daily changes in the environment. Such circadian organization demands at least a two-tier regulation of clock outputs; while the core clock resident in the SCN regulates SCN function and coordinates slave oscillators resident in the periphery, the peripheral oscillators regulate the specific function relevant to their tissue or organ function. Therefore, the determination of the full complement of mammalian genes under the control of the circadian oscillator will require systematic analysis of temporal gene expression in multiple organs.

Clock Gene Regulation of Transcription

To test whether the core circadian transcriptional activator, CLOCK (Gekakis et al., 1998; King et al., 1997), was involved in the regulation of most of the circadianly regulated output genes, we analyzed gene expression of *Clock* mutant mice at a time when CLOCK/MOP3 transcriptional activity is normally at its peak. The *Clock* mutant allele is an antimorph (a type of dominant-negative mutation) that antagonizes transcription induced by the CLOCK/MOP3 activator complex. At the behavioral level, these mice exhibit a lengthened endogenous period and become arrhythmic in complete darkness (Vitaterna et al., 1994). We hypothesized that transcripts that are downregulated in *Clock*/*Clock* mice would potentially be direct targets of the CLOCK protein. Furthermore, downregulated transcripts that normally share *Per2*-phased expression are likely targets of a CLOCK/MOP3 heterodimer binding at an E box element present in their structural genes. A direct comparison of gene expression between wild-type (wt) and *Clock*/*Clock* mice at zeitgeber time (ZT) 8, a time of maximal CLOCK/MOP3 transcriptional activity (Young and Kay, 2001), revealed 97 probe sets showing at least a 2-fold change in expression level (56 downregulated and 41 upregulated in the mutant). Surprisingly, only nine of these transcripts were cycling in the livers of wild-type mice, suggesting that *Clock* may be involved in processes other than circadian transcriptional regulation. The extensive transcriptional disruption in the *Clock*/*Clock* mutant mice is similar to the effect of the *jrk* mutation in flies in that transcriptional targets of dCLOCK are wide ranging beyond circadian outputs (Claridge-Chang et al., 2001; McDonald and Rosbash, 2001). Of these nine putative targets of CLOCK, seven transcripts were reduced in the mutant, including *Per2*, and most cycled in phase with *Per2* (Figure 2A). Conversely, the two remaining transcripts could be repressed either indirectly or potentially directly by CLOCK itself.

Another line of evidence that could indicate CLOCK regulation of target genes would be the identification of a CLOCK/MOP3 binding site in their candidate promoter regions (Hogenesch et al., 1998). To accomplish this, we took advantage of the recently available mammalian genome sequences (Lander et al., 2001; Venter et al., 2001). To enrich for conserved response elements, we searched for the presence of the CACGTGA sequence in genomic sequence 5′ of the start of translation in both the mouse and human genomes. Of the nearly 650 cycling genes identified by microarray, we were able to unambiguously retrieve the sequences of 127 genes from both species. Surprisingly, only nine genes harbored a CLOCK/MOP3 binding site in both species, including *Per2* and *Tubb5* (Figure 2B). Although this may reflect the fact that enhancer elements can occur at other locations than 5′ of the start methionine, a relatively small number of cycling promoters harbor obvious CLOCK binding sites. This observation is consistent with the results derived from the gene expression profiling of the *Clock*/*Clock* mutant mice and suggests that the circadian oscillator interacts with transcriptional networks underlying tissue-specific gene expression to orchestrate cycling transcription of separate sets of genes in different tissue types.

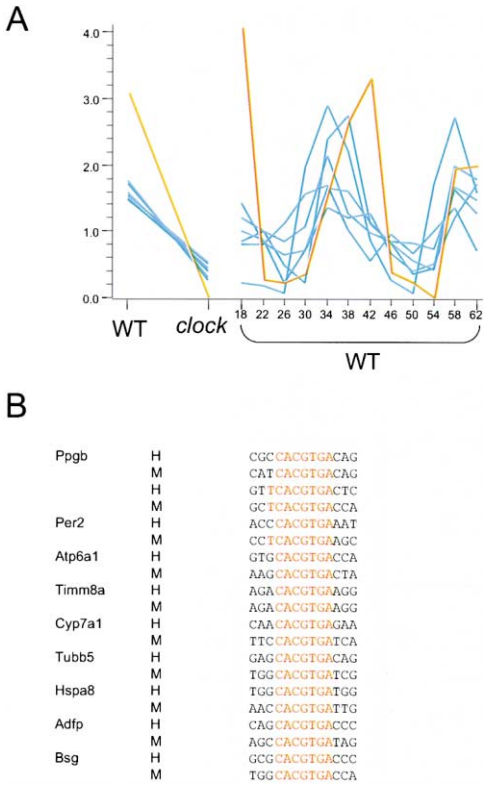

Figure 2. Regulation of Circadian Output Genes by *Clock*

(A) The expression pattern of cycling liver transcripts whose steady-state levels are suppressed by the *Clock* mutation were derived (see Supplemental Table S5). The temporal expression patterns of these genes under free running conditions in wild-type mice and the transcript levels in both mutant and wild-type livers at ZT8 (roughly equivalent to CT32 of free running condition) are shown. *Per2* expression is in orange.

(B) A search for the CLOCK/MOP3 binding site in 10kb 5′ upstream regions of 127 circadianly regulated mouse genes and their respective human homologs retrieved nine genes with this sequence conserved in both species. The core consensus site from each gene is indicated along with flanking nucleotides. When two sites were found in a single promoter region, both are indicated. Gene names are derived from Refseq (Pruitt et al., 2000).

Circadian Control of Organ Functions

To relate circadian-regulated transcripts with cellular physiology and organ function, we annotated the cycling genes and organized them into distinct pathways and functions. Such analysis revealed that a large proportion of circadianly regulated genes are implicated in functions specific to the SCN or liver.

Circadian Gene Regulation in the SCN

In mammals, the SCN is the anatomical site of a master circadian oscillator that imparts a daily rhythm in locomotor activity and associated physiologies such as feeding and metabolism. The SCN is thought to accomplish this by generating rhythms in various signaling cascades via both neural projections and possibly by diffusible factors, ultimately leading to the generation of organism-level rhythmic behaviors and physiologies. Major functions of the SCN, including protein/neuropeptide synthesis, processing, and degradation, as well as regulation of redox state and energy utilization, were all found to be circadianly regulated (Figures 3–5).

We also found cycling of a number of genes involved in pathways already experimentally linked to the circadian control of locomotor activity by the SCN. For example, we found that *Rgs16* and *Eps15* are circadianly regulated. These proteins are phosphorylated by the EGF receptor (Derrien and Druey, 2001; Fazioli et al., 1993), which has recently been implicated in circadian regulation of mouse locomotor activity (Kramer et al., 2001). We also found transcriptional cycling of neuronal nicotinic receptor b2 (*Chrnb2*), the mouse homolog of a gene mutated in the human disorder nocturnal frontal lobe epilepsy (De Fusco et al., 2000; Phillips et al., 2001). This suggests a possible role for *Chrnb2* in rhythmic control of motor coordination.

While the detailed pathways relating function of the above-mentioned genes to locomotor activity rhythms are yet to be described, transcripts for several well-defined prohormones and peptide neurotransmitters were also found to cycle in the SCN. They include proopiomelanocortin (*Pomc*), pituitary adenylate cyclase-activating polypeptide 1 (*Pacap*), cholecystokinin, and PDGF. Additional molecules, such as arginine-vasopressin (*Avp*), vasopressin receptor-α, somatostatin, enkephalin, galanin, and calcitonin gene-related peptide (*Cgrp*), have previously been reported to cycle at the mRNA levels in the SCN (Ibata et al., 1999). We also observed rhythms in the mRNA levels of genes involved in biosynthesis of nonpeptide neurotransmitters such as GABA and histamine (glutamic acid decarboxylase 1 [*Gad1*], histidine decarboxylase [*Hdc-c*]), as well as a large number of genes implicated in synthesis, processing, and release of neuropeptides and neurotransmitters.

Peptide Synthesis, Processing, and Secretion. The largest group of coordinately cycling transcripts in the SCN is involved in protein synthesis. More than 20 transcripts representing cytoplasmic ribosomal protein components and 13 representing mitochondrial ribosomal proteins showed coordinate cycling with a peak phase of expression at CT22 in the SCN but not liver (Figures 3A and 3B). The control points in ribosome biogenesis and the half-lives of ribosomes themselves exhibit great variability with tissue types (Kimball and Jefferson, 1994). SCN neurons may have adopted a temporal component of ribosome turnover to enhance neuropeptide/protein synthesis at particular circadian time points. In support of this hypothesis, diurnal changes in morphology and size of nucleoli in the rat supraoptic

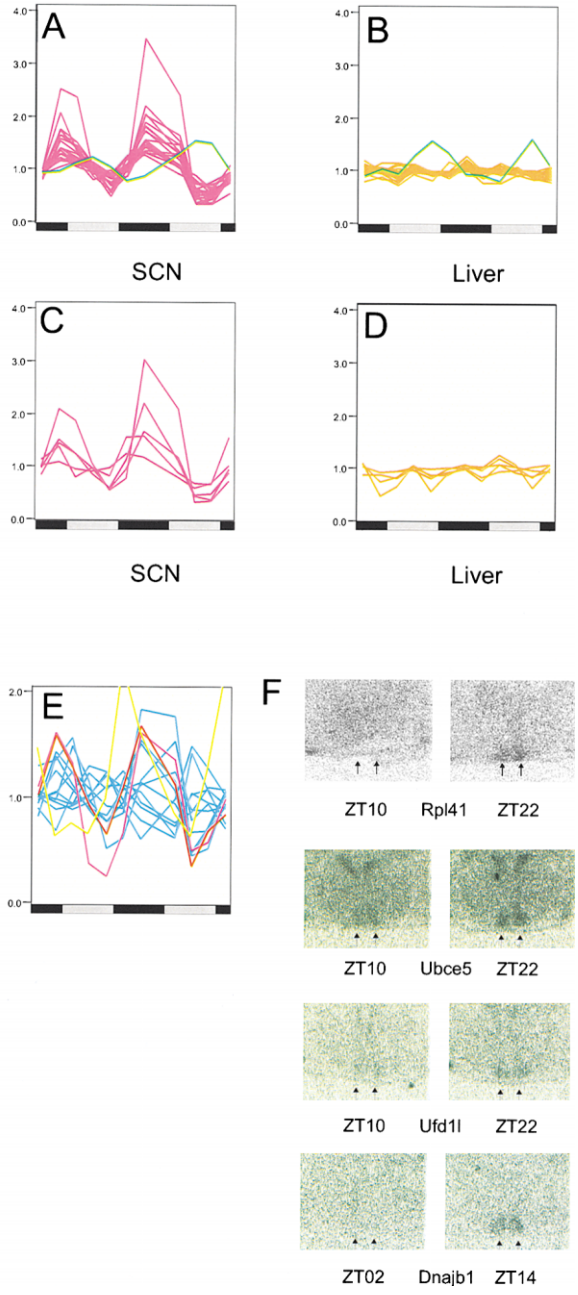

Figure 3. Circadian Regulation of Components of Protein Turnover in the SCN

Transcripts for ribosomal proteins (SCN, violet; liver, orange) and *Sui1* (green) (A and B) and protein processing components (*Nac*-α, *Srp14*, *Srp9*, *Sec61*-γ) (C and D) peak during night in the SCN (A and C) but not in liver (B and D). (E) Genes involved in protein folding and proteasome-mediated protein degradation (Supplemental Table S6) are circadianly regulated in the SCN. Cycling of *Ubce5* (red), *Ufd1l* (magenta), and *Dnajb1* (yellow) were confirmed by in situ hybridization in the SCN at peak and trough levels of expression (F). Cycling of the *Rpl41* transcript was also confirmed by in situ hybridization (F). Arrows indicate the SCN.

nucleus and superior cervical neurons have previously been observed (Bessone and Seite, 1985; Seite and Pebusque, 1985).

Several genes involved in steps subsequent to translation were also found to be circadianly regulated. Shortly after initiation of translation, two different cytoplasmic complexes, a dimeric nascent polypeptide-associated complex (NAC) and a multimeric ribonucleoprotein complex signal recognition particle (SRP), compete for binding to the nascent polypeptide exiting the ribosome (Raden and Gilmore, 1998). The SRP selects signal-containing ribosomes for targeting, while binding of the NAC prevents targeting of signal peptideless nascent chains to the endoplasmic reticulum (ER) membrane (Raden and Gilmore, 1998). Once the SRP binds to and docks proper ribosomes to the ER, the subsequent step of protein translocation requires the trimeric Sec61p complex. Oligomers of the Sec61 complex form a transmembrane channel where proteins are translocated across and integrated into the ER membrane (Jungnickel and Rapoport, 1995). The Sec61 complex has also been implicated in the translocation of misfolded proteins from the ER to the cytosolic protein degrading machinery, thereby ensuring folding of newly synthesized proteins with fidelity (Romisch, 1999). Constituents of the NAC (*Naca*), SRP (*Srp9*, *Srp14*), and Sec61 (β and γ) complexes exhibited coordinated transcriptional cycling (Figure 3C) in phase with the ribosomal cluster. In this manner, the circadian oscillator in the SCN coordinates protein synthesis and processing to the night, while no rhythm in these transcripts was detected in the liver (Figures 3B and 3D).

In order for the protein products of transcriptionally regulated genes to have a circadian rhythm, their synthesis and degradation must be tightly regulated. To begin to identify candidates for such regulation, we examined our circadianly regulated transcripts for components of protein folding and ubiquitin-mediated protein degradation pathways. *Dnajb1*, a member of DnaJ family (HSP40) of chaperonins, is circadianly regulated in the SCN (Figures 3E and 3F), while *Dnaja1* and *Dnajb6* cycle in the liver. Many proteins are degraded in a process in which ubiquitination facilitates their recognition and degradation via the proteasome. Some of these proteins are targeted for such degradation via their interaction with F box-containing proteins (del Pozo and Estelle, 2000). Nearly 12 genes coding for F box-containing proteins, ubiquitin-like proteins, ubiquitin-conjugating enzymes, ubiquitin fusion degradation-like proteins, and proteasomal subunits (Figure 3E; see Supplemental Table S6 at http://www.cell.com/cgi/content/full/109/3/307/DC1) were found to be circadianly regulated. Peak phases of expression of these genes are distributed throughout the circadian cycle, which may facilitate targeted degradation of specific proteins at different circadian times. It is important to note that cycling steady-state mRNA level may not always result in cycling protein levels. There are examples of genes whose mRNAs cycle, although their protein levels do not. Conversely, certain protein products cycle even though their transcripts do not (e.g., *lark* and *pdf* from *Drosophila*) (Newby and Jackson, 1993; Renn et al., 1999). In sum, concerted action of ribosome biogenesis and translation and protein processing, folding, and degradation may ultimately accentuate cycling levels of a large number of proteins including neuropeptides.

An important group of circadian output genes in the SCN includes proteins involved in neurosecretory processes and signaling. Coordinated expression of transcripts from genes involved in prohormone processing, vesicle transport and fusion, and late endosomal processing occurred during the anticipation of dawn and dusk (Figures 4A–4C). *Sgne1*, a secretory granule protein that activates prohormone convertase 2 (*Pcsk2*) (Braks and Martens, 1994), exhibits a circadian rhythm in its transcript expression. *Pcsk2* has been previously implicated in the processing of several neuropeptides including somatostatin (Mackin et al., 1991), an inhibitory neurotransmitter that is itself circadianly regulated to the same phase as *Sgne1*. *Sgne1*, therefore, may be accentuating the circadian expression of somatostatin, resulting in a protein rhythm with a peak at CT4 (Shinohara et al., 1991). Another secretory granule protein, secretogranin III (*Scg3*), also exhibits circadian regulation (Figure 4C).

Several components involved in vesicle trafficking are circadianly regulated to two distinct phases. AP4-sigma, involved in *trans*-golgi cycling (Hirst et al., 1999); *synapsin 1*, implicated in maintenance of a release-ready pool of presynaptic vesicles (Li et al., 1995); and *Vps29*, involved in recycling components from the endosome to the trans-golgi (Seaman et al., 1997), all cycle in phase with *Sgne1* and somatostatin. In contrast, *Snap25* and *Munc18c* (Jahn, 2000), which mediate vesicle fusion; *Eps15*, implicated in vesicle recycling (Salcini et al., 2001); and *Vps4b*, involved in late endosomal vesicle transport (Yoshimori et al., 2000), cycle with a peak in the late subjective day, CT10 (Figures 4A and 4B). Finally, we found cycling transcription of the mammalian ortholog of *Drosophila Slo*, *Kcnma1* (Figures 4D and 4E), that functions as a calcium-activated potassium channel and is believed to play a critical role in control of neurosecretion (Lara et al., 1999; Lovell and McCobb, 2001). In *Drosophila*, both *Slo* and a channel activity upmodulator, *Slob*, cycle in the head (Claridge-Chang et al., 2001; McDonald and Rosbash, 2001). Fly strains carrying mutations in *Slob* are behaviorally arrhythmic, implying a role of this potassium channel in circadian regulation of activity (Ceriani et al., submitted). These observations suggest that circadian regulation of neurotransmission occurs both at the level of secretory control factors, peptide hormones, and neurotransmitters themselves, and underscores the importance of neurosecretion as a primary mechanism of SCN control over peripheral circadian activity.

Redox and Energy Flux in the SCN. Several genes involved in energy production exhibit circadian rhythms in their steady-state mRNA levels in the SCN. These genes code for components involved in carbon utilization, oxidative phosphorylation, and the interconversion of nucleotide triphosphates. The transcripts of three major enzymes involved in carbon utilization, hexokinase1 (*Hk1*), malate dehydrogenase, and mitochondrial 3-ketoacyl-coa thiolase, cycle in the SCN with a peak expression at CT22, consistent with previous observations that 2-deoxyglucose utilization exhibits a marked circadian oscillation (Schwartz and Gainer, 1977). Hexokinase 1 and malate dehydrogenase mediate the use of glucose

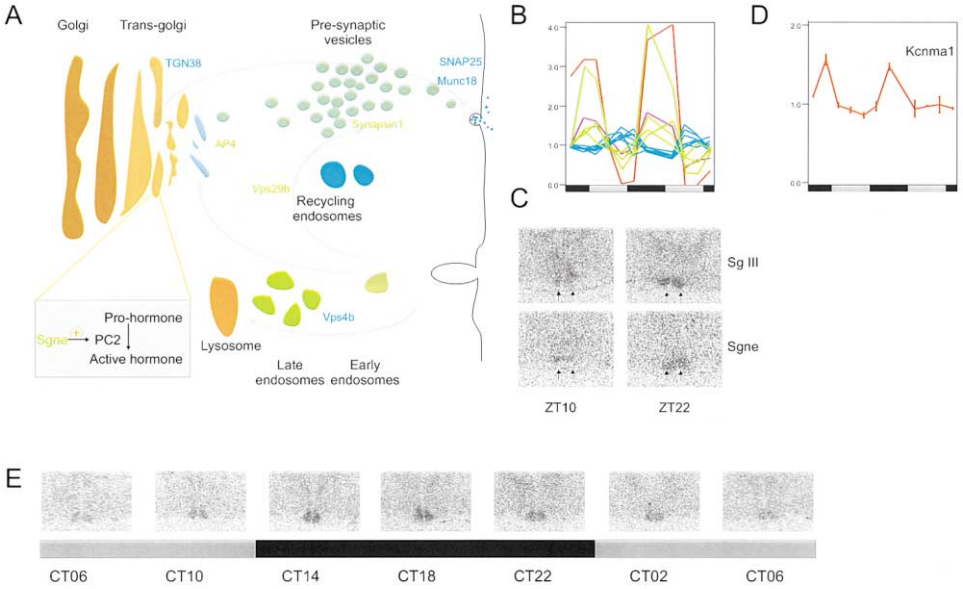

Figure 4. Circadian Expression of Vesicle Trafficking Components and of *Kcnma1* in the SCN

(A) Cycling genes along with their suggested function in different stages of vesicle transport are indicated. Color-matched data traces of cycling transcripts are shown in (B). Also shown are the traces of *Sgne1* in orange and somatostatin in green.
(C) In situ hybridization signals of *Sgne1* at the peak and trough levels of its expression supports cycling.
(D) The transcript for the voltage-dependent potassium channel *Kcnma1* cycles in the SCN.
(E) In situ hybridization signals of the *Kcnma1* transcript also exhibit cycling to the appropriate phase.

as an energy source, and mitochondrial 3-ketoacyl-coa thiolase regulates the use of ketone bodies—the major energy source in neurons. Reducing power derived from the breakdown of glucose and ketone bodies is ultimately used in mitochondrial oxidative phosphorylation to generate ATP and subsequently other NTPs. More than 20 components of the multisubunit mitochondrial complexes mediating oxidative phosphorylation and a nucleotide diphosphate kinase (*ndk3*) mediating interconversion of ATP and GTP are coordinately regulated and peak at CT22, perhaps anticipating the diurnal burst of neuronal activity (Figures 5A and 5B; Welsh et al., 1995). Such tight circadian coordination of the mitochondrial oxidative phosphorylation pathway may suggest a rhythm in redox state of the SCN neurons.

Circadian Gene Regulation in the Liver

The liver is the largest solid organ of the body and through its central role in metabolism and energy production, it significantly affects the physiological status of the organism. It receives blood supply from the portal vein as well as from hepatic arteries. The portal veins supply a wide range of nutrients, xenobiotics, and pathogenic elements from the digestive system, while the hepatic arteries supply a variety of endobiotic compounds including cytokines, metabolites, and hormones. The major functions of the liver include the metabolism of nutrients, endobiotics, and xenobiotics, the production of many ligands and cofactors, and the production of several serum proteins, which serve as the first line of defense against pathogenic particles. We found circadian regulation of many genes implicated in these major functions of the liver.

Nutrient Metabolism. Coordinated circadian expression of glucose transporters, the glucagon receptor, and enzymes involved in rate-limiting steps in the metabolism of hexose sugars were observed with a peak phase of expression in early evening (Figures 6A and 6B), the time when most feeding occurs in nocturnal rodents. In

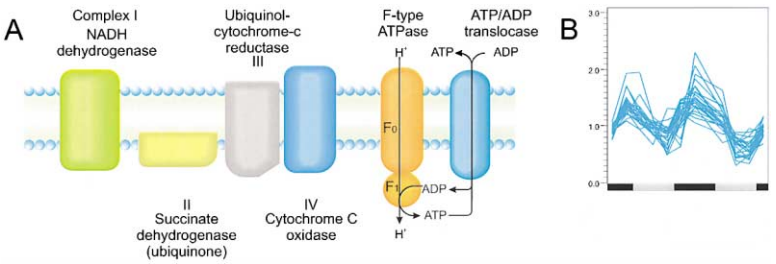

Figure 5. Circadian Regulation of Components of Oxidative Phosphorylation in the SCN

(A) Mitochondrial oxidative phosphorylation or the transfer of electrons from NADH to molecular oxygen with concomitant ATP production occurs in the mitochondrial membrane in four separate multisubunit complexes. The resulting proton-motive force is used by the multi subunit F-type ATPases to generate ATP from ADP. Components of these complexes are encoded by both the mitochondrial and nuclear genomes.

(B) At least seven nuclear components of complex I, one each of complexes II and III, and six of complex IV, as well as three components of the F-type ATPase, and mitochondrial ADP/ATP translocase 2 (Supplemental Table S6) peak during the subjective night.

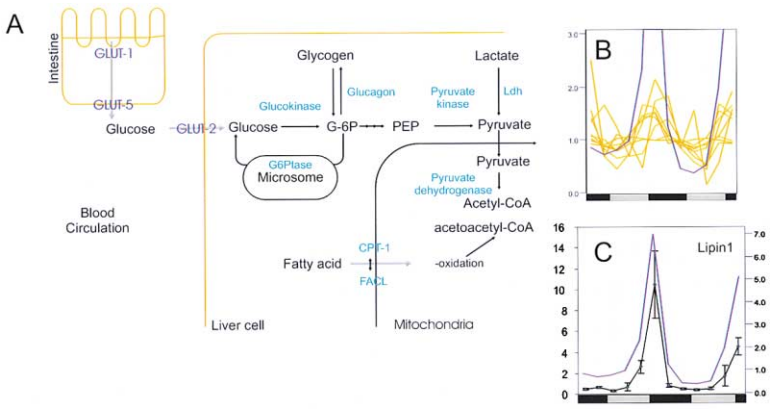

Figure 6. Circadian Regulation of Components of Energy Metabolism in Liver

(A) An overview of glucose and fatty acid metabolism in the liver. Cycling transcripts coding for enzymes and transporters are shown in blue.

(B) Components of gluconeogenesis, glycolysis, and fatty acid metabolism peak during the night when the animals consume the majority of their diet. *Glut1* and *Glut5* are known to cycle in the intestine during the night (Rhoads et al., 1998; Castello et al., 1995).

(C) A putative regulator of fatty acid utilization, lipin 1 (Peterfy et al., 2001) also cycles with a peak expression during day. Cycling of lipin 1 from the microarray data set (in purple and 2nd *y* axis) was also confirmed by real-time PCR (in black).

concert, these genes may facilitate glycogen synthesis during feeding and the use of hexose sugars as a primary energy source for several hours in the postadsorptive period (Arias et al., 2001). Circadian control of sugar-utilizing components (*Glut2*, glucose-6-phosphatase transport protein 1, pyruvate kinase, glucagon receptor) may constitute the underlying molecular bases of circadian control in glucose uptake and insulin response in rodents (la Fleur et al., 2001). In addition, we found cycling of lipin1, thought to be infolved in the regulation of sugar and lipid metabolism, and recently found mutated in a mouse model of human familial lipodystrophy (fld) (Figure 6; Peterfy et al., 2001). Similarly, the circadian oscillator facilitates the use of short- and medium-chain fatty acids during nighttime feeding and of stored very long-chain fatty acids during the day. This temporal orchestration may optimize the use of absorbed nutrients for energy generation and storage during feeding, and a switch to stored and alternative energy sources during fasting. Circadian regulation of energy metabolism in the liver may have implications in energy storage diseases.

Intermediate Metabolism. The liver is the major site of intermediate metabolism including the synthesis and degradation of cholesterol and the production of many ligands and cofactors. Cellular cholesterol homeostasis is maintained by the coordinated action of biosynthetic and degradative enzymes, transporters, and receptors (Figure 7; Ioannou, 2001). Niemann-Pick C1 (*Npc1*) plays a critical role in the intracellular trafficking of salvaged cholesterol from the late endosome to the trans-Golgi network; patients carrying a mutant *NPC1* gene develop a condition with high cholesterol levels in the endosomal-lysosomal system (Carstea et al., 1997). Transcript levels of *Npc1*, as well as of enzymes in the cholesterol biosynthetic pathway, exhibited a circadian rhythm (Figure 7B). De novo cholesterol biosynthesis starts with the conversion of acetoacetyl CoA to 3-hydroxy-3-methylglutaryl-CoA (HMGCoA). Subsequent conversion of HMGCoA to mevalonate by HMGCoA reductase (*Hmgcr*) is rate limiting and has long been known to be clock regulated in mammals (Shapiro and Rodwell, 1969). In addition to transcriptional regulation of *Hmgcr*, we found four other enzymes in the cholesterol synthetic pathway that exhibited coordinated cycling in their transcription (Figure 7B). This coordinated cycling of several biosynthetic enzymes in a single pathway may ensure a tighter circadian regulation of cholesterol production, or potentially may indicate that circadian regulation of the intermediates in the cholesterol synthetic pathway is important. While the timing of cholesterol synthesis is directed to the subjective day (when dietary cholesterol supply is low), the degradation products of cholesterol, steroids and biles, are produced at different times of the day (Figures 7A and 7C). Reflective of this, transcripts of many cytochrome P450s and enzymes involved in cholesterol catabolism (Kornmann et al., 2001) were found to be circadianly regulated and phased to the appropriate time of their utilization (Figures 7C and 7D).

The liver is the only organ that converts cholesterol to bile acids, and it uses a set of enzymes with broad substrate specificity for the breakdown and excretion of cholesterol and of many xenobiotics. These enzymes play a critical role in determining the bioactivity of drugs and their in vivo half-lives. This process occurs in two phases, with the first phase consisting of side group oxidation and hydroxylation and the second involving the addition of a polyatomic group such as sulfate, glutathione, glucuronate, or an amino acid such as glycine or taurine (Arias et al., 2001). These processes change the bioactive properties of many substrates and enhance their solubility at acidic pH. We found circadian regulation of transcripts for more than 10 cytochrome P450s and related genes mediating the phase I oxidation of cholesterol (Figures 7A and 7E). Synthesis of conjugation partners, such as taurine and glycine, or enzymes of the second phase biotransformation, such as GST, was also found to be under circadian control. For example, we found cycling of cysteine dioxygenase (*Cdo*). *Cdo* catalyzes reduction of cysteine to 3-sulfinoalanine, which is subsequently metabolized to taurine and sulfite (Michal, 1999).

Xenobiotic metabolism has long been known to depend on the time of day (Lake et al., 1976). One important mechanism for this metabolism is methylation, as it alters the activity of many xenobiotics. Four methyltransferases exhibited circadian rhythms in their transcript levels: betaine-homocysteine methyl transferase (*Bhmt*), nicotinamide N-methyltransferase (*Nnmt*), thioether S-methyltransferase (*Temt*), and thiopurine methyltransferase (*Tpmt*). Importantly, the activities of most methyltransferases are fine-tuned by the cellular concentration

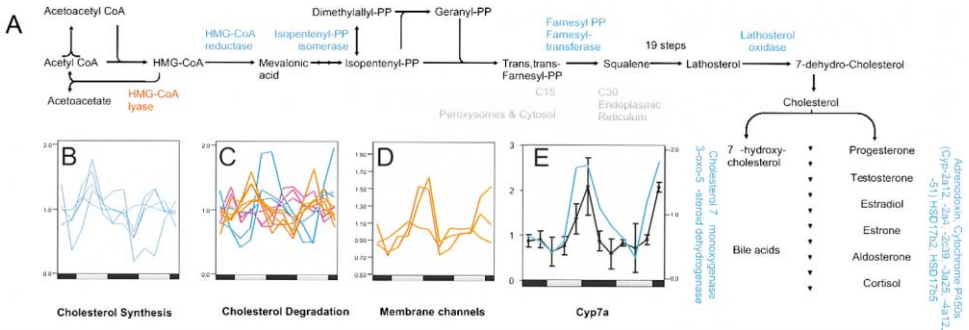

Figure 7. Circadian Regulation of Cholesterol Metabolism in Liver

(A) An overview of the cholesterol synthetic pathway in animals (Michal, 1999). Reactions from 3-carbon acetyl CoA up to 15-carbon (C_{15}) trans-trans farnesyl-PP take place in the peroxisome and cytosol. Steps after the circadianly regulated condensation of two C_{15} units to form squalene proceed on the ER. Degradation of cholesterol produces different steroids, and finally bile acids.

(B) Enzymes of cholesterol biosynthesis (in blue) peak during the night.

(C) Enzymes of cholesterol degradation peak at different times of the day.

(D) Transcripts of three membrane channels, *Mrp2*, *Slc22a1*, and *Slc22a2*, which transport bile acids and organic cations, also cycle.

(E) Cycling of *Cyp7a* (in blue) was confirmed by real-time PCR (black).

of S-adenosylhomocysteine (SAH) (Michal, 1999). We observed cycling transcript levels of SAH hydrolase, which catalyzes the reversible hydrolysis of SAH to adenosine and L-homocysteine and regulates the intracellular SAH concentration. Finally, conjugated bile acids and biotransformed xenobiotics are excreted from hepatocytes by different membrane transporters, some of which (*Slc22a1*, *Slc22a2*, and *Mrp2*) were found to be cycling (Figure 7D). The organic cation transporters *Slc22a1* and *Slc22a2* transport choline and polyamines, while substrates for *Mrp2* include bile acid conjugates, glutathione-, glucuronate-, and anionic conjugates of both endobiotics and xenobiotics (Arias et al., 2001; Kullak-Ublick et al., 2000). Circadianly regulated transcription of components of xenobiotic metabolism and excretion may account for observed chronotoxicity and bioavailability of a large number of drugs and drug metabolites (Focan, 1995).

The liver is the major site of synthesis of many bioactive molecules, such as nuclear receptor ligands, polyamines, cofactors, and the oxygen carrier heme. For example, the thyroid gland releases inactive thyroxine (T4) into blood circulation, which is subsequently deionized to the active T3 form by the liver enzyme deiodinase1 (*Dio1*). Circadianly regulated synthesis and release of T4 from the thyroid has long been considered the underlying mechanism in maintaining a daily rhythm in serum T3. This proposed mechanism, however, fails to explain a daily rhythm of plasma T3 in hypothyroidism patients receiving exogenous T4 (Burr et al., 1975). Cycling hepatic transcript levels of *Dio1* in our data set may better explain the above clinical observation. Synthesis of the nuclear receptor ligand retinoic acid and of the visual photopigment retinol from all-*trans*-retinal may also be under circadian control, as transcript levels of two enzymes, retinol dehydrogenase 7 (*Rdh7*) and retinal short-chain dehydrogenase/reductase-1 (*Rsdr1*-pending), cycle. These two enzymes act upon all-*trans*-retinal produced in a one-step reaction from dietary β carotene (that comes from plants).

Immune Mechanisms. The liver is also a major site of synthesis of many immunologically important plasma proteins. Transcript levels of agents of innate immunity, such as mannan binding lectin serine protease 1 (*Masp1*), mannose binding lectin (*Mbl2*), and proinflammatory protein phospholipase A2, exhibited a circadian rhythm in their steady-state mRNA levels. Binding of *Mbl2* or *Masp1* to high mannose and N-acetylglucosamine oligosaccharides present on a variety of microorganisms activates *Masp1*, which in turn recruits C4 and C2 complement proteins to trigger the lectin pathway of the complement cascade (Michal, 1999). Transcripts of both *Mbl2* and *Masp1* cycle with a peak expression level around late afternoon, perhaps preparing the body for an encounter with bacterial pathogens in the early hours of activity and feeding.

A number of components of coagulation and fibrinolytic pathways are synthesized in liver. Although circadian regulation of coagulation and fibrinolytic activities has been described in humans (Andreotti and Kluft, 1991; Labrecque and Soulban, 1991), we observed a transcriptional rhythm in several key regulators previously unknown to cycle. Factors such as tissue factor pathway inhibitor 2 (*Tfpi2*), heparin cofactor II (*Serpind1*), α-2 antiplasmin (*Serpinf2*), and α-2 macroglobulin all displayed a pronounced circadian rhythm in their steady-state mRNA levels. *Tfpi2* is a regulator of the extrinsic pathway of blood coagulation through its ability to inhibit factor Xa and TF-VIIa activity. Formation of TF-VIIa complex is the triggering event in the coagulation cascade. *Tfpi2* inhibition of TF-VIIa activity prevents initiation of the coagulation cascade if the triggering stimulus is too weak (Michal, 1999). Heparin cofactor II is one of the plasma cofactors required for the anticoagulant property of heparin. α-2 antiplasmin and α-2 macroglobulin are plasmin inhibitors and are thought to be important in the regulation of fibrinolysis in vivo. Alpha-2 macroglobulin also has an anticoagulation effect by binding and sequestering the free protein C available for coagulation (Michal, 1999). Transcript levels of these four key inhibitors of coagulation and fibrinolysis cycle with a peak phase of expression during the (behaviorally inactive) day.

The circadian oscillator in nocturnal rodents consoli-

dates feeding and phases it to the night. This raises a possibility that circadian transcriptional regulation in the liver may be a result of both cell-autonomous circadian clock and feeding-associated gene expression. Recent evidence has shown that circadianly regulated genes exhibit differences in their expression under restricted and ad libitum feeding regimens, suggesting that feeding is a component of rhythmicity in normal (driven) conditions (Kita et al., 2002).

Circadian Control of Rate-Limiting Steps

Examination of the function of circadianly regulated genes in the SCN and liver revealed that major functions of both structures are under circadian control. In the regulation of physiology, an efficient mechanism for regulation of a pathway is to exert control at biochemically rate-limiting steps. Circadian control of many pathways and processes in these two tissues occurs at key rate-limiting steps, some of which are discussed here.

The first and rate-limiting step in ribosome biogenesis in nucleoli is the synthesis of ribosomal RNAs mediated by the multisubunit RNA polymerase-I and its accessory factors (Larson et al., 1991). While none of the core RNA PolI subunits exhibited any significant transcriptional rhythm in the SCN, a component shared by all three RNA polymerases—metallothionein 1 activator—did exhibit a rhythm in peak phase with the ribosomal protein transcripts. Transcriptional control of a common subunit of all three polymerases may ensure coordinated regulation of both rRNA and r-protein transcription. Additionally, transcript levels of *TAFIb*, a part of the SL1 complex that recruits RNA PolI to the rRNA promoters, and of topoisomerase I, essential for RNA PolI-mediated transcription (Larson et al., 1991), cycle in similar phases.

In the SCN, circadian control of genes mediating key steps in processing of neuropeptides (*Sgne1*) and synthesis of neurotransmitters (*Gad1* and *Hdc-c*) may ultimately generate a circadian variation in their neurotransmission. Finally, cycling transcript levels for several channel proteins and receptors (*Clcn4-2*, *Cacna2d3*, *Clcn3*, *Slc8a1*, *Kcnma1*, *Avpr1a*, *Calcr*, *Crcp*, *Chrnb2*, and *Cckar*) may be an effective mechanism in generating circadian variation in neuronal signaling.

The rate-limiting nature of many cycling genes in the liver is even more apparent. The liver, as the major site of metabolism, also handles a significant flux of metabolites across membranes. Circadian regulation of several membrane channels and transporters (*Slc10a1*, *Slc22a1*, *Slc27a2*, *Slc2a2*, *Slc7a2*, *Abcc2*, and *Aqp9*), allowing substrate and product movement across membranes, may be an effective mechanism for temporal sequestration of metabolites. Cycling transcript levels of several key components in nutrient and intermediate metabolism, discussed in the previous sections, may offer additional levels of control.

Within a species, important physiological processes may be regulated across tissues, but the mechanisms may reflect their distinct physiologies. For example, while we observed the circadian regulation of genes regulating sugar metabolism in both the SCN and liver, the points of regulation are different. SCN neurons primarily utilize hexose sugars as energy sources to maintain the electrochemical gradient and to generate ATP. Therefore, tight circadian regulation of energy sources (*Hk1*) and their use at the terminal oxidative phosphorylation step (several components of mitochondrial oxidative phosphorylation) is an effective mechanism. Sugar metabolism in the liver is more variable as intermediate products are themselves used to produce bioactive molecules. Therefore, the circadian control of sugar metabolism in the liver is more elaborate, including the initial steps of glucose utilization (*G6pt1*) as well as several intermediate steps that may serve as starting points for the generation of intermediate metabolites (for example, pyruvate kinase and fumarate hydratase).

Furthermore, as key pathways are conserved across species, the circadian regulation of the rate-limiting steps in these pathways is likewise conserved. Circadian regulation of some of these rate-limiting steps in more divergent species such as plants indicates that nature may have devised circadian regulation of key biochemical steps as an effective mechanism for temporal regulation of physiology and behavior. For example, fidelity in translational initiation is largely dependent on proper initiation complex formation. One key regulator of this process is *Sui-1* (Cui et al., 1998), first identified in yeast. *Sui-1* transcript levels cycle in the SCN, the liver, as well as in *Arabidopsis* and *Drosophila* (Ceriani et al., submitted; Harmer et al., 2000). A second example is HMGCoA metabolism, where the rate-limiting enzyme in plants, HMGCoA lyase, is under circadian control in plants, while in flies, rats, and mice, HMGCoA reductase is rate limiting and circadianly regulated (Ceriani et al., submitted; Harmer et al., 2000; Kita et al., 2002). Additional examples are found in the heme biosynthetic pathway and in the metabolism of β carotene. The first committed and physiologically irreversible step in heme biosynthesis is the condensation of glycine and succinyl coenzyme A to yield aminolevulinic acid (ALA). Circadian control of ALA-synthase1 (*Alas1*) transcription in flies and mammals and of many additional enzymes in the subsequent reactions in plants (Ceriani et al., submitted; Harmer et al., 2001; Zheng et al., 2001) is a demonstration of circadianly regulated production of a cellular redox sensor across species. Finally, while in mice metabolism of β carotene to produce retinoic acid and the visual photopigment retinal is clock regulated, in plants, a putative β carotene hydroxylase that converts β carotene to zeaxanthine and related photo-protective pigments xanthophylls is also under circadian control (Harmer et al., 2000; Michal, 1999). The circadian metabolism of β carotene is therefore conserved across species, demonstrating evolutionary pressure in regulated synthesis of major light-sensing pigments in both plants and animals.

Summary

We present a global analysis of circadian patterns of transcription from the core pacemaker in the SCN and from an important physiological mediator and peripheral oscillator, the liver. Importantly, we find that circadian regulation of a majority of genes is tissue specific, and only a small subset of these genes are direct targets of the transcription factors driving the core oscillator. Because the vast majority of cycling genes in both SCN and liver are specific to those tissues, we suggest that

the profiling of additional tissues and organs may eventually reveal that up to 10% of the mammalian transcriptome may be under circadian control.

In each tissue type examined, the major clusters of circadianly regulated genes participate in the principal functions of the organ, and many are the rate-limiting steps in their respective pathways. The peak phases of expression of these key transcripts are also appropriately timed. A comparison of circadian transcription in mammals and flies (Claridge-Chang et al., 2001; McDonald and Rosbash, 2001; Ceriani et al., submitted) suggests that circadian control of several key processes and pathways including heme biosynthesis (*Alas1*), cholesterol metabolism (*HMGCoA lyase*), neuropeptide signaling (*Dbi*), neuronal excitability (*Kcnma1/slo*), energy metabolism (*hexokinase*), and xenobiotic metabolism (*glutathione-s-transferase* and *cytochrome p450s*) have been conserved over more than 600 million years of evolution. The circadian control of transcription in higher organisms is integrated with the spatial control of gene expression to target rate-limiting steps in major pathways in their relevant organs, resulting in a systems-level temporal orchestration of behavior and physiology for optimal adaptation of the organism to its environment.

Experimental Procedures

Animals

One hundred twenty male C57BL/6J mice of 7–8 weeks of age were purchased from the Jackson Laboratory and maintained for two weeks on a LD12:12 cycle in the Northwestern University Center for Comparative Medicine. All animal care and use procedures followed approved institutional guidelines. After placing in constant darkness (DD), ten animals were sacrificed every four hours, beginning at hour 30 of DD for two complete 24 hr cycles (second and third cycle in DD). Mice were sacrificed by cervical dislocation, and the optic nerves were cut in complete darkness using an infrared viewer (FJW Industries, Palatine, IL). Brain dissections were performed under dim red illumination (15W Kodak safe lamp filter 1A). The SCN was quickly dissected under bright-light illumination using a dissecting microscope, placed in a 5 μl drop of TRIZOL reagent (Invitrogen, Carlsbad, CA) sitting on aluminum foil, and rapidly frozen on dry ice. Ten individual SCNs frozen in TRIZOL were pooled and stored at −80°C until RNA extraction. Livers were rapidly frozen on dry ice and stored at −80°C. Total liver RNA for real-time PCR was extracted using TRIZOL reagent according to manufacturer's protocol. Three samples were used for each time point. Total RNA used for real-time PCR and Affymetrix probe preparation was extracted from livers of the same animals. To study the effects of the *Clock* mutation on gene expression profiles in liver, three wild-type and three *Clock* mutant C57BL/6J male mice were entrained to LD12:12 as above and their livers were collected at ZT8.

Probe Hybridization

Total RNA was prepared, and samples were labeled and hybridized in duplicate (or more) to mouse (U74A) high-density oligonucleotide arrays as previously described (Lockhart et al., 1996; Sandberg et al., 2000; Wodicka et al., 1997). For each time point, either 10 μg (liver) or 30 ng (SCN) of total RNA were used as starting material. For the SCN samples, cRNA obtained in the first round of synthesis (without biotin label) was used in a second round of cRNA synthesis (with biotin label) to produce enough probe for hybridization. Primary image analysis of the arrays was performed using the Genechip 3.2 software package (Affymetrix, Santa Clara, CA), and images were scaled to an average hybridization intensity (average difference value) of 200.

Data Analysis for Identification of Cycling Genes

To define circadianly expressed transcripts, we used a statistical program COSOPT based on an algorithm we previously described (Harmer et al., 2000). COSOPT imports data and calculates the mean expression intensity and its corresponding standard deviation (SD). It then performs an arithmetic linear regression detrend of the original time series. The mean and SD of the detrended time series are then calculated. COSOPT does not standardize the linear-regression detrended time series to standard normal deviates, as did CORCOS, thus allowing COSOPT to quantitatively assess oscillatory amplitude more directly. Variable weighting of individual time points (as in SEMs from replicate measurements) can be accommodated during analysis for the presence of rhythms in terms of a user-specified number and range of periods (test periods spaced uniformly in period space). Specifically, for each test period, 101 test cosine basis functions (of unit amplitude) are considered varying over a range of phase values from plus one-half the period to minus one-half the period (i.e., such that phase is considered in increments of 1% of each test period). For each test cosine basis function, COSOPT calculates the least-squares optimized linear correspondence between the linear regression-detrended data, ylr(x), and the test cosine basis function, yb(x), as a function of x [i.e., such that the approximation of ylr(x) by the test cosine basis function, yb(x), is optimized across all values, x, in terms of two parameters, ALPHA and BETA, whereby ylr(x)∼ALPHA+BETA*yb(x)]. The quality of optimization possible by the test cosine basis function is quantitatively characterized by the sum of squared residuals between ylr(x) and the approximation given by [ALPHA+BETA*yb(x)] (referred to as CHI2, for chi-squared). The values of CHI2 are used to identify the phase at which the optimal correspondence between ylr(x) and yb(x) is obtained for each test period (i.e., the phase giving the smallest CHI2 value corresponds to the optimal phase). Thus, for each test period, ALPHA, BETA, and CHI2 are assessed at the optimal phase. Note that, interpretively, BETA now represents an optimized, parametrized measure of the magnitude of the oscillatory amplitude expressed by ylr(x) (in relation to, or as modeled by, a cosine wave of the corresponding period and optimal phase). One thousand Monte Carlo cycles are carried out in which surrogate realizations of ylr(x) are generated by both (1) randomly shuffling temporal sequence and (2) adding pseudo-Gaussian-distributed noise to each surrogate point in proportion to the corresponding value of point uncertainty (i.e., replicate SEM). In this way, specifically accounted for in the surrogate realizations are both (1) the influence of temporal patterning and (2) the magnitude of point-wise experimental uncertainty. Then, as with the original ylr(x) sequence, optimal values of ALPHA and BETA are determined, along with a corresponding CHI2, and retained in memory for each surrogate at each test period/optimal phase. For each test period/optimal phase, the mean and standard deviation of the surrogate BETA values are then calculated. These values, in relation to the BETA value obtained for the original ylr(x) series, are then used to calculate a one-sided significance probability based on a normality assumption (which is in fact satisfied by the distribution of BETA values obtained from the 1000 randomized surrogates). A summary of the analytical session is then produced for each time series, composed of entries for only those test periods that correspond to CHI2 minima, the best phase and the MMC-β value describing the goodness of fit.

Data Analysis for *Clock* Mutant Mice

Replicate chip hybridization data from wild-type and *Clock* mutant mice liver were analyzed by ANOVA. Probe sets showing at least a 2-fold difference in expression levels and a p-ANOVA score of 0.05 or less were considered significant.

Search for E Box Elements

Probe sets for all cycling genes were mapped to Unigene using BLAST (Altschul et al., 1990) as previously described (Hogenesch et al., 2001). The first 300 coding nucleotides of each complete Unigene cluster harboring a translational methionine was used as bait sequences to search the Celera Mouse and Human Assemblies (R12 masked and R26b, respectively) using BLAST as above. Hits were indexed up to 10 kb upstream of the translational methionine (when available) and used to find the consensus CLOCK/MOP3

binding site, CACGTGA. Where the element was found in the putative promoter sequences from both species, it is reported.

In Situ Hybridization

C57BL/6J male mice were entrained to LD12:12 for at least 1 week before brain collection. Six mice per probe were sacrificed at the appropriate zeitgeber time (ZT) for peak and trough expression as determined by the microarray data. Brains were rapidly dissected and frozen on dry ice. Alternate 20 μm coronal sections through the SCN were thaw-mounted on gelatin-coated slides. In situ hybridization was performed as described in Sangoram et al. (1998). 36-mer synthetic oligonucleotide probes (Integrated DNA Technology, Inc.) for *Ufd1l*, *Ubce5*, *SgIII*, *Sgne*, *Kcnma1*, *Rpl41*, *Rev-erb* β, *Dnajb1*, and *Per2* were ^{33}P-3′-labeled using terminal l Deoxynucleotidyl Transferase (GIBCO-BRL). Slides were hybridized at 37°C overnight in a solution containing1X Denhart's, 4X SSC, 50 μg/ml polyadenylitic acid, 500 μg/ml sheared salmon sperm DNA, 10% dextran sulfate, 50% deionized formamide, and 2 nM of the appropriate probe. Image analysis was performed with NIH Image v1.62 (http://rsb.info.nih.gov/nih-image/).

Real-Time PCR

RNA quantitation was performed using a fluorescence-based real-time PCR technology (TaqMan Real-Time PCR, Applied Biosystems, Foster City, CA; Gibson et al., 1996; Heid et al., 1996). The following probes and primers were designed using ABI PrimerExpress software: *Per2*-For, GCC TTC AGA CTC ATG ATG ACA GA; *Per2*-Rev, TTT GTG TGC GTC AGC TTT GG; *Per2*-Probe, ACT GCT CAC TAC TGC AGC CGC TCG T; Rev-erb-β (U09504)-For, GGC AAG GCA ACA CCA AGA A; Rev-erb-β-Rev, GGC CGC TGC GTC CAT; Rev-erb-β Probe, GTT CTG GCA TGT CCC ATG AAC ATG; Rev-erb α-For, TCC TGG CAT GAC TAA GAG TCA CA; Rev-erb α-Rev, GCC ACA TCC CCA CAG ACT TT; Rev-erb α-Probe, TGG AAT GAC AAA ATT TAG TGG CAT GGT TCT ACT G; Lipin1-Probe, AGA CGG AAA TGC AGT TTG TGA ACG AGG; Lipin-For, ACT GCT CAT CCA CCA GAG TAA GG; Lipin-Rev, CCC CCA AGG ACT CGA GAT C; *Bhlhb2*-FOR, GTG CAT TGC CCA GCT GAA G; *Bhlhb2*-REV, CTC CAG AAC CAC TGC TTT TTC C; *Bhlhb2*-Probe, CCG AAC ATC TCA AAC TTA CTA CTT TGG GTC ACT TG; *Cyp7a*-For, CCA TGA TGC AAA ACC TCC AAT; *Cyp7a*-Rev, ACC CAG ACA GCG CTC TTT GA; *Cyp7a1*-Probe, TGT CAT GAG ACC TCC GGG CCT TCC; *Ldh1*-For, CAC ATC CTG GGC CAT TGG; *Ldh1*-Rev, GCA CCC GCC TAA GGT TGT TC; *Ldh1*-Probe, TCT GTG GCA GAC TTG GCT GAG AGC AT. All probes were 5′-labeled with FAM (6-carboxyfluorescein) and 3′-labeled with TAMRA (6-carboxytetramethylrhodamine). To eliminate the possibility of contaminating genomic DNA amplification, both probe sequences were designed to cross exon junctions in the corresponding cDNA sequences. Of each total RNA sample, 25–100 ng was used in a 25 μl RT-PCR reaction according to the manufacturer's protocol (Perkin Elmer TaqMan EZ RT-PCR Kit) with appropriate primers and probes. For control reactions, mouse GAPDH mRNA was amplified from the same RNA samples using the Rodent GAPDH Control Reagent Kit (VIC Probe, ABI). PCR conditions were optimized for probe and primer concentrations so that the target and control reactions were performed in the same tube using the following thermal cycling parameters: 50°C for 2 min, 60°C for 30 min, and 95°C for 5 min, followed by 40 two-step cycles of 94°C for 20 s and 62°C for 1 min. Relative mRNA abundance was calculated using the comparative delta-Ct method. All final measurements were normalized by the target mRNA/GAPDH average value for all samples.

Acknowledgments

This work is supported by the Novartis Research Foundation, the National Science Foundation (NSF) Center for Biological Timing, and the National Institute of Mental Health (NIMH #MH51573). J.S.T. is an Investigator in the Howard Hughes Medical Institute. B.H.M. is the recipient of an NSF Graduate Research Fellowship. The authors would like to thank Keith Ching for his annotation of genes represented on the arrays. The authors would like to acknowledge Drs. Martha Vitaterna and Lisa Wilsbacher for assistance with tissue collection and Jennifer Villasenor for her excellent technical assistance. The authors would like to thank Drs. Joel Kreps, Stacey Harmer, Tony Orth, Trey Sato, and Fernanda Ceriani for helpful comments on the manuscript.

Received: February 12, 2002
Revised: March 28, 2002
Published online: April 2, 2002

References

Altschul, S.F., Gish, W., Miller, W., Myers, E.W., and Lipman, D.J. (1990). Basic local alignment search tool. J. Mol. Biol. *215*, 403–410.

Andreotti, F., and Kluft, C. (1991). Circadian variation of fibrinolytic activity in blood. Chronobiol. Int. *8*, 336–351.

Arias, I.M., Boyer, J.L., Chisari, F.V., Fausto, N., Schachter, D., and Shafritz, D.A. (2001). The Liver: Biology and Pathophysiology, 4th Edition (Philadelphia, PA: Lippincott Williams & Wilkins).

Bessone, R., and Seite, R. (1985). Daily fluctuations of nucleoli in neurosecretory cells of the rat supraoptic nucleus. An ultrastructural and stereological study. Cell Tissue Res. *240*, 393–396.

Braks, J.A., and Martens, G.J. (1994). 7B2 is a neuroendocrine chaperone that transiently interacts with prohormone convertase PC2 in the secretory pathway. Cell *78*, 263–273.

Burr, W.A., Black, E.G., Griffiths, R.S., and Hoffenberg, R. (1975). Serum triiodothyronine and reverse triiodothyronine concentrations after surgical operation. Lancet *2*, 1277–1279.

Carstea, E.D., Morris, J.A., Coleman, K.G., Loftus, S.K., Zhang, D., Cummings, C., Gu, J., Rosenfeld, M.A., Pavan, W.J., Krizman, D.B., et al. (1997). Niemann-Pick C1 disease gene: homology to mediators of cholesterol homeostasis. Science *277*, 228–231.

Castello, A., Guma, A., Sevilla, L., Furriols, M., Testar, X., Palacin, M., and Zorzano, A. (1995). Regulation of GLUT5 gene expression in rat intestinal mucosa: regional distribution, circadian rhythm, perinatal development and effect of diabetes. Biochem. J. *309*, 271–277.

Claridge-Chang, A., Wijnen, H., Naef, F., Boothroyd, C., Rajewsky, N., and Young, M.W. (2001). Circadian regulation of gene expression systems in the *Drosophila* head. Neuron *32*, 657–671.

Cui, Y., Dinman, J.D., Kinzy, T.G., and Peltz, S.W. (1998). The Mof2/Sui1 protein is a general monitor of translational accuracy. Mol. Cell. Biol. *18*, 1506–1516.

De Fusco, M., Becchetti, A., Patrignani, A., Annesi, G., Gambardella, A., Quattrone, A., Ballabio, A., Wanke, E., and Casari, G. (2000). The nicotinic receptor beta 2 subunit is mutant in nocturnal frontal lobe epilepsy. Nat. Genet. *26*, 275–276.

del Pozo, J.C., and Estelle, M. (2000). F-box proteins and protein degradation: an emerging theme in cellular regulation. Plant Mol. Biol. *44*, 123–128.

Derrien, A., and Druey, K.M. (2001). RGS16 function is regulated by epidermal growth factor receptor-mediated tyrosine phosphorylation. J. Biol. Chem. *276*, 48532–48538.

Fazioli, F., Minichiello, L., Matoskova, B., Wong, W.T., and Di Fiore, P.P. (1993). eps15, a novel tyrosine kinase substrate, exhibits transforming activity. Mol. Cell. Biol. *13*, 5814–5828.

Focan, C. (1995). Circadian rhythms and cancer chemotherapy. Pharmacol. Ther. *67*, 1–52.

Gekakis, N., Staknis, D., Nguyen, H.B., Davis, F.C., Wilsbacher, L.D., King, D.P., Takahashi, J.S., and Weitz, C.J. (1998). Role of the CLOCK protein in the mammalian circadian mechanism. Science *280*, 1564–1569.

Gibson, U.E., Heid, C.A., and Williams, P.M. (1996). A novel method for real time quantitative RT-PCR. Genome Res. *6*, 995–1001.

Grundschober, C., Delaunay, F., Puhlhofer, A., Triqueneaux, G., Laudet, V., Bartfai, T., and Nef, P. (2001). Circadian regulation of diverse gene products revealed by mRNA expression profiling of synchronized fibroblasts. J. Biol. Chem. *276*, 46751–46758.

Harmer, S.L., Hogenesch, J.B., Straume, M., Chang, H.S., Han, B., Zhu, T., Wang, X., Kreps, J.A., and Kay, S.A. (2000). Orchestrated transcription of key pathways in *Arabidopsis* by the circadian clock. Science *290*, 2110–2113.

Harmer, S.L., Panda, S., and Kay, S.A. (2001). Molecular bases of circadian rhythms. Annu. Rev. Cell Dev. Biol. *17*, 215–253.

Heid, C.A., Stevens, J., Livak, K.J., and Williams, P.M. (1996). Real time quantitative PCR. Genome Res. *6*, 986–994.

Hirst, J., Bright, N.A., Rous, B., and Robinson, M.S. (1999). Characterization of a fourth adaptor-related protein complex. Mol. Biol. Cell *10*, 2787–2802.

Hogenesch, J.B., Gu, Y.Z., Jain, S., and Bradfield, C.A. (1998). The basic-helix-loop-helix-PAS orphan MOP3 forms transcriptionally active complexes with circadian and hypoxia factors. Proc. Natl. Acad. Sci. USA *95*, 5474–5479.

Hogenesch, J.B., Ching, K.A., Batalov, S., Su, A.I., Walker, J.R., Zhou, Y., Kay, S.A., Schultz, P.G., and Cooke, M.P. (2001). A comparison of the Celera and Ensembl predicted gene sets reveals little overlap in novel genes. Cell *106*, 413–415.

Ibata, Y., Okamura, H., Tanaka, M., Tamada, Y., Hayashi, S., Iijima, N., Matsuda, T., Munekawa, K., Takamatsu, T., Hisa, Y., et al. (1999). Functional morphology of the suprachiasmatic nucleus. Front. Neuroendocrinol. *20*, 241–268.

Ioannou, Y.A. (2001). Multidrug permeases and subcellular cholesterol transport. Nat. Rev. Mol. Cell. Biol. *2*, 657–668.

Jahn, R. (2000). Sec1/Munc18 proteins: mediators of membrane fusion moving to center stage. Neuron *27*, 201–204.

Jungnickel, B., and Rapoport, T.A. (1995). A posttargeting signal sequence recognition event in the endoplasmic reticulum membrane. Cell *82*, 261–270.

Kimball, S.R., and Jefferson, L.S. (1994). Mechanisms of translational control in liver and skeletal muscle. Biochimie *76*, 729–736.

King, D.P., and Takahashi, J.S. (2000). Molecular genetics of circadian rhythms in mammals. Annu. Rev. Neurosci. *23*, 713–742.

King, D.P., Zhao, Y., Sangoram, A.M., Wilsbacher, L.D., Tanaka, M., Antoch, M.P., Steeves, T.D., Vitaterna, M.H., Kornhauser, J.M., Lowrey, P.L., et al. (1997). Positional cloning of the mouse circadian clock gene. Cell *89*, 641–653.

Kita, Y., Shiozawa, M., Jin, W., Majewski, R.R., Besharse, J.C., Greene, A.S., and Jacob, H.J. (2002). Implications of circadian gene expression in kidney, liver and the effects of fasting on pharmacogenomic studies. Pharmacogenetics *12*, 55–65.

Kornmann, B., Preitner, N., Rifat, D., Fleury-Olela, F., and Schibler, U. (2001). Analysis of circadian liver gene expression by ADDER, a highly sensitive method for the display of differentially expressed mRNAs. Nucleic Acids Res. *29*, E51.

Kramer, A., Yang, F.C., Snodgrass, P., Li, X., Scammell, T.E., Davis, F.C., and Weitz, C.J. (2001). Regulation of daily locomotor activity and sleep by hypothalamic EGF receptor signaling. Science *294*, 2511–2515.

Kullak-Ublick, G.A., Beuers, U., and Paumgartner, G. (2000). Hepatobiliary transport. J. Hepatol. *32*, 3–18.

Labrecque, G., and Soulban, G. (1991). Biological rhythms in the physiology and pharmacology of blood coagulation. Chronobiol. Int. *8*, 361–372.

la Fleur, S.E., Kalsbeek, A., Wortel, J., Fekkes, M.L., and Buijs, R.M. (2001). A daily rhythm in glucose tolerance: a role for the suprachiasmatic nucleus. Diabetes *50*, 1237–1243.

Lake, B.G., Tredger, J.M., Burke, M.D., Chakraborty, J., and Bridges, J.W. (1976). The circadian variation of hepatic microsomal drug and steroid metabolism in the golden hamster. Chem. Biol. Interact. *12*, 81–90.

Lander, E.S., Linton, L.M., Birren, B., Nusbaum, C., Zody, M.C., Baldwin, J., Devon, K., Dewar, K., Doyle, M., FitzHugh, W., et al. (2001). Initial sequencing and analysis of the human genome. Nature *409*, 860–921.

Lara, J., Acevedo, J.J., and Onetti, C.G. (1999). Large-conductance Ca2+-activated potassium channels in secretory neurons. J. Neurophysiol. *82*, 1317–1325.

Larson, D.E., Zahradka, P., and Sells, B.H. (1991). Control points in eucaryotic ribosome biogenesis. Biochem. Cell Biol. *69*, 5–22.

Li, L., Chin, L.S., Shupliakov, O., Brodin, L., Sihra, T.S., Hvalby, O., Jensen, V., Zheng, D., McNamara, J.O., Greengard, P., et al. (1995). Impairment of synaptic vesicle clustering and of synaptic transmission, and increased seizure propensity, in synapsin I-deficient mice. Proc. Natl. Acad. Sci. USA *92*, 9235–9239.

Liu, Y., Tsinoremas, N.F., Johnson, C.H., Lebedeva, N.V., Golden, S.S., Ishiura, M., and Kondo, T. (1995). Circadian orchestration of gene expression in cyanobacteria. Genes Dev. *9*, 1469–1478.

Lockhart, D.J., Dong, H., Byrne, M.C., Follettie, M.T., Gallo, M.V., Chee, M.S., Mittmann, M., Wang, C., Kobayashi, M., Horton, H., and Brown, E.L. (1996). Expression monitoring by hybridization to high-density oligonucleotide arrays. Nat. Biotechnol. *14*, 1675–1680.

Lorent, K., Overbergh, L., Delabie, J., Van Leuven, F., and Van den Berghe, H. (1994). Distribution of mRNA coding for alpha-2-macroglobulin, the murinoglobulins, the alpha-2-macroglobulin receptor and the alpha-2-macroglobulin receptor associated protein during mouse embryogenesis and in adult tissues. Differentiation *55*, 213–223.

Lovell, P.V., and McCobb, D.P. (2001). Pituitary control of BK potassium channel function and intrinsic firing properties of adrenal chromaffin cells. J. Neurosci. *21*, 3429–3442.

Mackin, R.B., Noe, B.D., and Spiess, J. (1991). Identification of a somatostatin-14-generating propeptide converting enzyme as a member of the kex2/furin/PC family. Endocrinology *129*, 2263–2265.

McDonald, M.J., and Rosbash, M. (2001). Microarray analysis and organization of circadian gene expression in Drosophila. Cell *107*, 567–578.

Michal, G. (1999). Biochemical Pathways (New York: John Wiley & Sons).

Newby, L.M., and Jackson, F.R. (1993). A new biological rhythm mutant of *Drosophila melanogaster* that identifies a gene with an essential embryonic function. Genetics *135*, 1077–1090.

Peterfy, M., Phan, J., Xu, P., and Reue, K. (2001). Lipodystrophy in the fld mouse results from mutation of a new gene encoding a nuclear protein, lipin. Nat. Genet. *27*, 121–124.

Phillips, H.A., Favre, I., Kirkpatrick, M., Zuberi, S.M., Goudie, D., Heron, S.E., Scheffer, I.E., Sutherland, G.R., Berkovic, S.F., Bertrand, D., and Mulley, J.C. (2001). CHRNB2 is the second acetylcholine receptor subunit associated with autosomal dominant nocturnal frontal lobe epilepsy. Am. J. Hum. Genet. *68*, 225–231.

Pruitt, K.D., Katz, K.S., Sicotte, H., and Maglott, D.R. (2000). Introducing RefSeq and LocusLink: curated human genome resources at the NCBI. Trends Genet. *16*, 44–47.

Raden, D., and Gilmore, R. (1998). Signal recognition particle-dependent targeting of ribosomes to the rough endoplasmic reticulum in the absence and presence of the nascent polypeptide-associated complex. Mol. Biol. Cell *9*, 117–130.

Renn, S.C., Park, J.H., Rosbash, M., Hall, J.C., and Taghert, P.H. (1999). A pdf neuropeptide gene mutation and ablation of PDF neurons each cause severe abnormalities of behavioral circadian rhythms in *Drosophila*. Cell *99*, 791–802.

Rhoads, D.B., Rosenbaum, D.H., Unsal, H., Isselbacher, K.J., and Levitsky, L.L. (1998). Circadian periodicity of intestinal Na+/glucose cotransporter 1 mRNA levels is transcriptionally regulated. J. Biol. Chem. *273*, 9510–9516.

Romisch, K. (1999). Surfing the Sec61 channel: bidirectional protein translocation across the ER membrane. J. Cell Sci. *112*, 4185–4191.

Salcini, A.E., Hilliard, M.A., Croce, A., Arbucci, S., Luzzi, P., Tacchetti, C., Daniell, L., De Camilli, P., Pelicci, P.G., Di Fiore, P.P., and Bazzicalupo, P. (2001). The Eps15 *C. elegans* homologue EHS-1 is implicated in synaptic vesicle recycling. Nat. Cell Biol. *3*, 755–760.

Sandberg, R., Yasuda, R., Pankratz, D.G., Carter, T.A., Del Rio, J.A., Wodicka, L., Mayford, M., Lockhart, D.J., and Barlow, C. (2000). Regional and strain-specific gene expression mapping in the adult mouse brain. Proc. Natl. Acad. Sci. USA *97*, 11038–11043.

Sangoram, A.M., Saez, L., Antoch, M.P., Gekakis, N., Staknis, D., Whiteley, A., Fruechte, E.M., Vitaterna, M.H., Shimomura, K., King, D.P., et al. (1998). Mammalian circadian autoregulatory loop: a timeless ortholog and mPer1 interact and negatively regulate CLOCK-BMAL1-induced transcription. Neuron *21*, 1101–1113.

Schwartz, W.J., and Gainer, H. (1977). Suprachiasmatic nucleus: use of 14C-labeled deoxyglucose uptake as a functional marker. Science *197*, 1089–1091.

Seaman, M.N., Marcusson, E.G., Cereghino, J.L., and Emr, S.D. (1997). Endosome to Golgi retrieval of the vacuolar protein sorting receptor, Vps10p, requires the function of the VPS29, VPS30, and VPS35 gene products. J. Cell Biol. *137*, 79–92.

Seite, R., and Pebusque, M.J. (1985). Chronobiological studies on the nucleolus. Chronobiol. Int. *2*, 69–91.

Shapiro, D.J., and Rodwell, V.W. (1969). Diurnal variation and cholesterol regulation of hepatic HMG-CoA reductase activity. Biochem. Biophys. Res. Commun. *37*, 867–872.

Shinohara, K., Isobe, Y., Takeuchi, J., and Inouye, S.T. (1991). Circadian rhythms of somatostatin-immunoreactivity in the suprachiasmatic nucleus of the rat. Neurosci. Lett. *129*, 59–62.

Su, A.I., Cooke, M.P., Ching, K.A., Hakak, Y., Walker, J.R., Wiltshire, T., Orth, A.P., Vega, R.G., Sapinoso, L.M., Moqrich, A., et al. (2002). Large-scale analysis of the human and mouse transcriptomes. Proc. Natl. Acad. Sci. USA, in press. Published online March 19, 2002. 10.1073/pnas.012025199.

Venter, J.C., Adams, M.D., Myers, E.W., Li, P.W., Mural, R.J., Sutton, G.G., Smith, H.O., Yandell, M., Evans, C.A., Holt, R.A., et al. (2001). The sequence of the human genome. Science *291*, 1304–1351.

Vitaterna, M.H., King, D.P., Chang, A.M., Kornhauser, J.M., Lowrey, P.L., McDonald, J.D., Dove, W.F., Pinto, L.H., Turek, F.W., and Takahashi, J.S. (1994). Mutagenesis and mapping of a mouse gene, Clock, essential for circadian behavior. Science *264*, 719–725.

Wang, Y., Osterbur, D.L., Megaw, P.L., Tosini, G., Fukuhara, C., Green, C.B., and Besharse, J.C. (2001). Rhythmic expression of Nocturnin mRNA in multiple tissues of the mouse. BMC Dev. Biol. *1*, 9.

Welsh, D.K., Logothetis, D.E., Meister, M., and Reppert, S.M. (1995). Individual neurons dissociated from rat suprachiasmatic nucleus express independently phased circadian firing rhythms. Neuron *14*, 697–706.

Wodicka, L., Dong, H., Mittmann, M., Ho, M.H., and Lockhart, D.J. (1997). Genome-wide expression monitoring in *Saccharomyces cerevisiae*. Nat. Biotechnol. *15*, 1359–1367.

Yoshimori, T., Yamagata, F., Yamamoto, A., Mizushima, N., Kabeya, Y., Nara, A., Miwako, I., Ohashi, M., Ohsumi, M., and Ohsumi, Y. (2000). The mouse SKD1, a homologue of yeast Vps4p, is required for normal endosomal trafficking and morphology in mammalian cells. Mol. Biol. Cell *11*, 747–763.

Young, M.W., and Kay, S.A. (2001). Time zones: a comparative genetics of circadian clocks. Nat. Rev. Genet. *2*, 702–715.

Zheng, B., Albrecht, U., Kaasik, K., Sage, M., Lu, W., Vaishnav, S., Li, Q., Sun, Z.S., Eichele, G., Bradley, A., and Lee, C.C. (2001). Nonredundant roles of the mPer1 and mPer2 genes in the mammalian circadian clock. Cell *105*, 683–694.

Zylka, M.J., Shearman, L.P., Weaver, D.R., and Reppert, S.M. (1998). Three period homologs in mammals: differential light responses in the suprachiasmatic circadian clock and oscillating transcripts outside of brain. Neuron *20*, 1103–1110.